Proceedings of the Institution of Civil Engineers
Water Management 000
Month 2008 Issue WM0
Pages 1–14
doi: 10.1680/wama.2008.000.0.1
Paper 700022
Received 02/06/2007
Accepted 28/01/2008
Keywords:
floods & floodworks/hydraulics & hydrodynamics/risk & probability analysis

Ben Gouldby
Principal Scientist,
HR Wallingford Ltd,
Wallingford,
Oxfordshire

Paul Sayers
Group Manager,
HR Wallingford Ltd,
Wallingford,
Oxfordshire

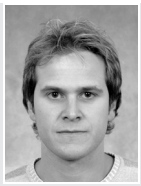

Jonatan Mulet-Marti
Mechanical Engineer,
Wallingford Software Ltd,
Oxfordshire

Mohamed Ahmed Ali Mohamed Hassan
Senior Numerical Modeller,
HR Wallingford Ltd,
Wallingford, Oxfordshire

Douglas Benwell
GIS Scientist,
HR Wallingford Ltd,
Wallingford,
Oxfordshire

A methodology for regional-scale flood risk assessment

B. Gouldby BSc, P. Sayers CEng, MICE, J. Mulet-Marti MSc, M. A. A. M. Hassan Phd and D. Benwell

Sound flood risk management decision-making is underpinned by flood risk analysis. Current methods applied at regional and local scales are often limited in their consideration of the potential for defences to fail. Ultimately this can lead to underestimates of the true risk and subsequent difficulties in justifying mitigation measures such as maintenance and replacement of defences. A methodology has been developed for assessing flood risk arising from fluvial and coastal sources that explicitly considers defence failures represented through fragility curves. This method requires consideration of flooding scenarios involving multiple defence section failures and flood events ranging in severity. It has therefore been necessary to develop a purpose-specific flood spreading method that is capable of simulating many flood events in practical timescales. The method has been applied to the Thames Estuary, where outputs including spatial maps of flood risk and defences attributed with residual risk have been used to support decisions relating to strategic flood risk management over the coming century.

NOTATION

A	sub-set of possible defence system states
a_l	number of elements of A under load l
c	economic consequence for a single flood event
D	Random variable for defence system state
d	defence system state
$d_1, d_2, \ldots, d_n$	defence sections 1, 2, …, n
$\overline{d}_i$	event: non-failure of defence section i
f_X	joint density of x
$G(\boldsymbol{X}) < 0$	exceedence of limit state function/s (failure region)
L	random variable for defence load
l	defence load
m_l	number of hydraulic model runs for load l
n	number of defences in the defence system
q	number of loading levels
R	impact cell flood risk (expected annual damage)
$v_1, v_2, \ldots, v_n$	volume discharged through defence section $1, 2, \ldots, n$
$\boldsymbol{X}$	vector of basic variables
Y	random variable for flood depth
y	flood depth
$z_1, z_2, \ldots, z_m$	impact cells 1, 2, …, m

1. INTRODUCTION

Recent serious flood events such as those experienced across Europe in 1998,[1] 2000[2] and more recently in New Orleans in 2005, highlighted the serious hazard posed by flooding. In the UK, decisions relating to flood management are increasingly being informed by risk-based methods.[3–6] These methods not only seek to quantify current flood risk but also to quantify changes in flood risk over short-, medium- and long-term timescales. The performance of flood management options relating to, for example, asset management and long-term planning can then be explored through the application of the methods and the results used to underpin rational decision making. Quantified flood risk analysis is, however, complex. Flooding can arise from different sources, extreme tidal surges or fluvial flows, for example, or these phenomena acting in tandem. With timescales of a century under consideration for strategic planning purposes, a changing climate further complicates analysis of these extreme events. Defences designed to reduce the impacts of flooding can and do fail.[7] Data relating to defence failures remain sparse and the processes that cause failures are often not well understood. It is necessary, however, to predict the change in failure likelihood, as a result of deterioration and maintenance interventions, over long timescales—a challenging task in its own right. Where floodplain topography is variable it is necessary to employ hydraulic models to determine the route of water flowing on to the floodplain from breached or overtopped defences; these can be computationally intensive to run[8] and, therefore, the number of scenarios that can be modelled is constrained. Traditional methods for regional flood risk assessment[9] assume failures do not occur and therefore underestimate the true risk. They also have simple flood spreading approaches, which further increases uncertainty on their outputs.

In order to combat this complexity and improve flood risk analyses, a hierarchical framework of methods is under development.[5] A national-scale method applied to England and Wales has recently identified the risk to property from fluvial and coastal flooding, expressed as an expected annual damage, to be £1·3 billion.[10] This national approach necessarily adopts a number of simplifications to keep the computational burden practical for this scale of analysis. At smaller spatial scales there is a requirement for more robust approaches to represent appropriately local features of defences and local flooding characteristics.

The current paper describes a flood risk method that expands upon recent work but is appropriate for regional-scale flood risk

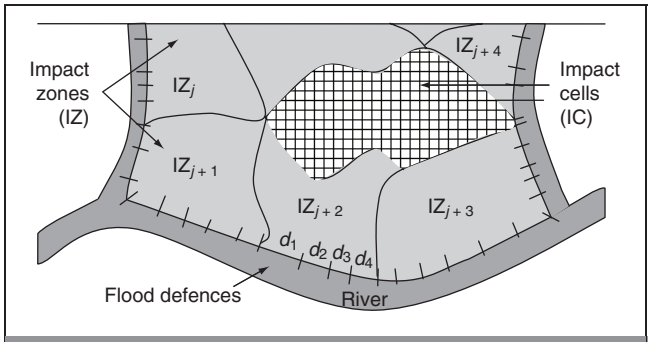

Fig. 1. Conceptual illustration of the modelled system

analysis. It can be used to inform decisions relating to long-term planning and maintenance prioritisation. The method incorporates defence reliability analysis and can include the effects of climate change as well as changes in floodplain use. The application of the method to the Thames Estuary is then detailed.

2. OVERVIEW OF METHODOLOGY

The modelled flood system, depicted in Fig. 1, shows a floodplain area protected from a river channel by a series of n discrete flood defences $(d_1, d_2, \ldots, d_n)$. Each defence section is considered to have an independent and different resistance to flood loading. These are characterised by, for example, different types of structure (i.e. different geometry or materials), crest levels or condition grades (Fig. 2). Defence section parameters, for example crest level, are assumed to be constant within any given section. Research has identified this assumption to be reasonable for defence lengths up to around 500 m,[11] longer defence lengths are therefore sub-divided. The floodplain area is discretised into a series of impact cells $(z_1, z_2, \ldots, z_m)$. Any specified impact cell can be affected by flood water discharged through any of the defences that protect it.

The hydraulic loads on the defences are defined as a continuous random variable (L) and characterised by extreme value distributions associated with each defence. Defence failure (structural failure) is defined as a continuous random variable, conditional on load (these distributions are often referred to as fragility curves[12]). During any flood event each individual defence section can exist in two possible states (i.e. they are defined as Bernoulli random variables), failed or not failed $(d_i, \bar{d}_i)$, with the likelihood of any particular state obtained with reference to the fragility curves.

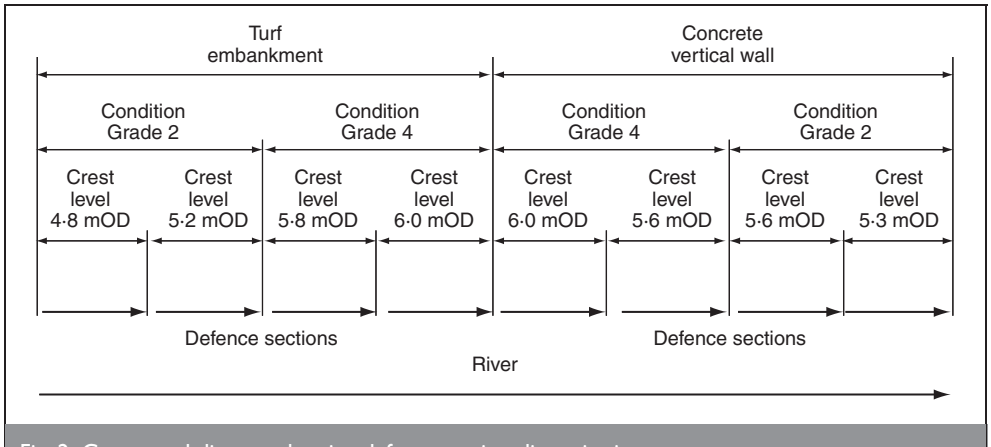

Fig. 2. Conceptual diagram showing defence section discretisation

The continuous line of defence sections forms a defence system. The defence system state is defined as a discrete random variable, D, whose value d, under any hydraulic load L, is a function of the (Bernoulli) state of each defence (i.e. d is a function of the vector whose elements comprise the (Bernoulli) state of each defence section). The potential number of defence system states (combinations of failed/not failed defences) and thereby the number of values that d can take on, for any specified hydraulic load (l), is 2^n. The conditional probability mass function of D is simply

$$p_{D|L}(d, l) = P[D = d \,|\, L = l] \quad (1)$$

The performances of consecutive defence lengths are assumed to be independent of one another, then the probability of any particular defence system state, for example, $d_1, \ldots, d_k, \bar{d}_{k+1}, \ldots, \bar{d}_n$, occurring on any given hydraulic load (l), is, through the multiplication rule

$$p_{D|L}(d, l) = P[D = d \,|\, L = l] = \prod_{i=1}^{k} p(d_i|l) \prod_{i=k+1}^{n} [1 - p(\bar{d}_i|l)] \quad (2)$$

Flood volumes discharged through (or over) any given defence section during any flood event are a function of the state of each defence section and therefore the defence system state. The random variable of flood depth, Y, in any impact cell is a function of the flood volume discharged into the floodplain during the flood event and thereby a function of the defence system state.

$$Y = g(D) \quad (3)$$

In order to determine the conditional event probability of exceeding any particular flood depth (y) in any particular impact cell during a flood event, involves enumeration of the probability mass function (equation (1)) for defence system states that yield flood depths greater than y (the set that contains these system states is denoted as A).

$$p(Y > y|l) = p[g(D) > y|l] = \sum_{A} p_{D|L}(d, l) \quad (4)$$

If the function that relates the defence system states to the flood depth is readily evaluated then the solution of equation (4) is simple. In practice, however, evaluation of this function involves running a hydraulic model, which is potentially computationally demanding, particularly given that the number of defences in a system can often exceed 100 (i.e. more than 2^{100} possible defence system states). The solution adopted to solve this problem is two-fold, comprising numerical approximation using a Monte Carlo technique coupled with a computationally efficient hydraulic flood spreading method.

The Monte Carlo simulation approach is initiated by generating M sets of n random numbers for a specified loading condition l. The random numbers are generated from a uniform distribution ranging between 0 and 1. The mapping from the random number set to the defence system state is obtained with reference to the loading event and the fragility curve. So, for example, if the probability of failure at loading level l is identified with reference to the fragility curve of a specific defence section as u, random numbers that are less than or equal to u translate to a defence failure, random numbers greater than u denote non-failure. Through this mapping, M defence system states are obtained. These system states, together with the hydraulic loads, form the basis for the boundary conditions of a hydraulic flood spreading model, which is used to simulate the M flood events. The conditional event probability of exceeding any particular flood depth in any given impact cell is now

$$p(Y > y|l) \approx \frac{a_l}{m_l} \quad (5)$$

where a_l is the number of elements within the set A (i.e. the number of system states that result in a flood depth greater than y) under the loading event l and m_l is the total number of hydraulic model simulations undertaken for that loading event.

In order to obtain the unconditional annual probability of exceeding y, the continuous loading distributions for each defence section are discretised into q levels of l: $l_1, l_2, l_3, \ldots, l_q$, under the assumption of dependent loads (i.e. the defences comprised within a flood area are assumed to be subjected to a load of equal recurrence interval, simultaneously), giving

$$p(Y > y) \approx \sum_{i=2}^{q-1} \left[\left[p\left(L \geqslant \frac{l_i + l_{i+1}}{2}\right) - p\left(L \geqslant \frac{l_i + l_{i-1}}{2}\right) \right] \frac{a_{l_i}}{m_{l_i}} \right] \quad (6)$$

In practice, the loading levels are associated with return periods and l is computed through consideration of the return period and number of events per year.[13] Typically 2 year to 10 000 year return period events cover a sufficient range of loading events.

With knowledge of the type, floor area and number of properties within each impact cell, it is possible to estimate the economic consequences owing to property damage (c).[14] Each modelled flood event (loading event and sampled defence system state) results in a flood depth grid over the floodplain area and hence a flood event economic damage. The mean economic consequence, conditional on the loading event, associated with an impact cell is obtained from

$$\overline{c}_l \approx \frac{1}{m_l} \sum_{j=1}^{m_l} c_j \quad (7)$$

The impact cell risk (R), expressed as expected annual damage (EAD), is then calculated using the same load discretisation procedure detailed in equation (6).

$$R \approx \sum_{i=2}^{q-1} \left[\left[p\left(L \geqslant \frac{l_i + l_{i+1}}{2}\right) - p\left(L \geqslant \frac{l_i + l_{i-1}}{2}\right) \right] \overline{c}_{l_i} \right] \quad (8)$$

The total risk for the flood area is the sum of the risk associated with each impact cell. The Monte Carlo sampling can be constrained through monitoring convergence on a specified quantity of interest. For example, where a precise estimate of the economic damage associated with a specific loading level is required, rather than the fully integrated risk (EAD), the defence system states are continuously sampled for each loading level and convergence is monitored on the mean event economic damage (equation (7)), prior to substitution into equation (8). If, however, the EAD is the quantity of interest, equation (8) is used to monitor the convergence. Defence system states are sampled consecutively for each loading level and the EAD is evaluated after a batch of M by q flood event simulations (equation (8)). The EAD is monitored for successive batches until convergence is reached. In practice, the convergence criteria are expressed in terms of variation of the absolute value of economic damage at each loading level or risk (EAD), depending on the study requirements. The former approach provides a mechanism for specifying a higher degree of accuracy for particular loading event economic damages. The latter method offers significantly higher computational efficiency while maintaining robustness, as the economic damages associated with loading levels that contribute little to the EAD are implicitly restricted (i.e. not necessarily converged). A flow diagram of the model calculations is shown in Fig. 3, further details of the primary components of the method are discussed below.

3. DERIVATION OF FRAGILITY CURVES

The method requires the performance of each individual flood defence section to be expressed in terms of failure probabilities that are conditional on loads. Ideally, local defence-specific studies that consider multiple defence failure mechanisms and parameters derived from local measurement will form the basis of the reliability calculations used in the derivation of the fragility curves.[15] At present it is, however, rare to find such information. A generic database containing over 600 fragility curves has therefore been developed for use where local information is unavailable.

The generic fragility curves are derived using traditional reliability methods.[16] In general terms, structural failure occurs when the defence loads exceed the resistance variables (collectively these loads and resistance variables are termed the basic variables). Structural failure mechanisms, which are functions of the basic variables (denoted by the vector $\boldsymbol{X}$), are termed limit state functions ($G(\boldsymbol{X})$). Probability distributions and parameters are assigned to the load and strength variables, the unconditional probability of failure is then determined through integration of the joint density function (f_X) of the loads and strengths over the region where the limit state is exceeded ($G(\boldsymbol{X}) \leqslant 0$), the so-called failure region[16]

$$p_f = P[(G(\boldsymbol{X}) \leqslant 0] = \int \cdots \int_{G(\boldsymbol{X}) \leqslant 0} f_X(\boldsymbol{X})\, d\boldsymbol{X} \quad (9)$$

Generally this integration cannot be performed analytically and two dominant approaches are used for its solution: transformation of the joint density of the basic variables to a multivariate normal probability density function and use of the known characteristics of this distribution (first- and second-order second moment (FORM and SORM) approaches[16]) and Monte Carlo methods. For the derivation of fragility curves, the traditional reliability

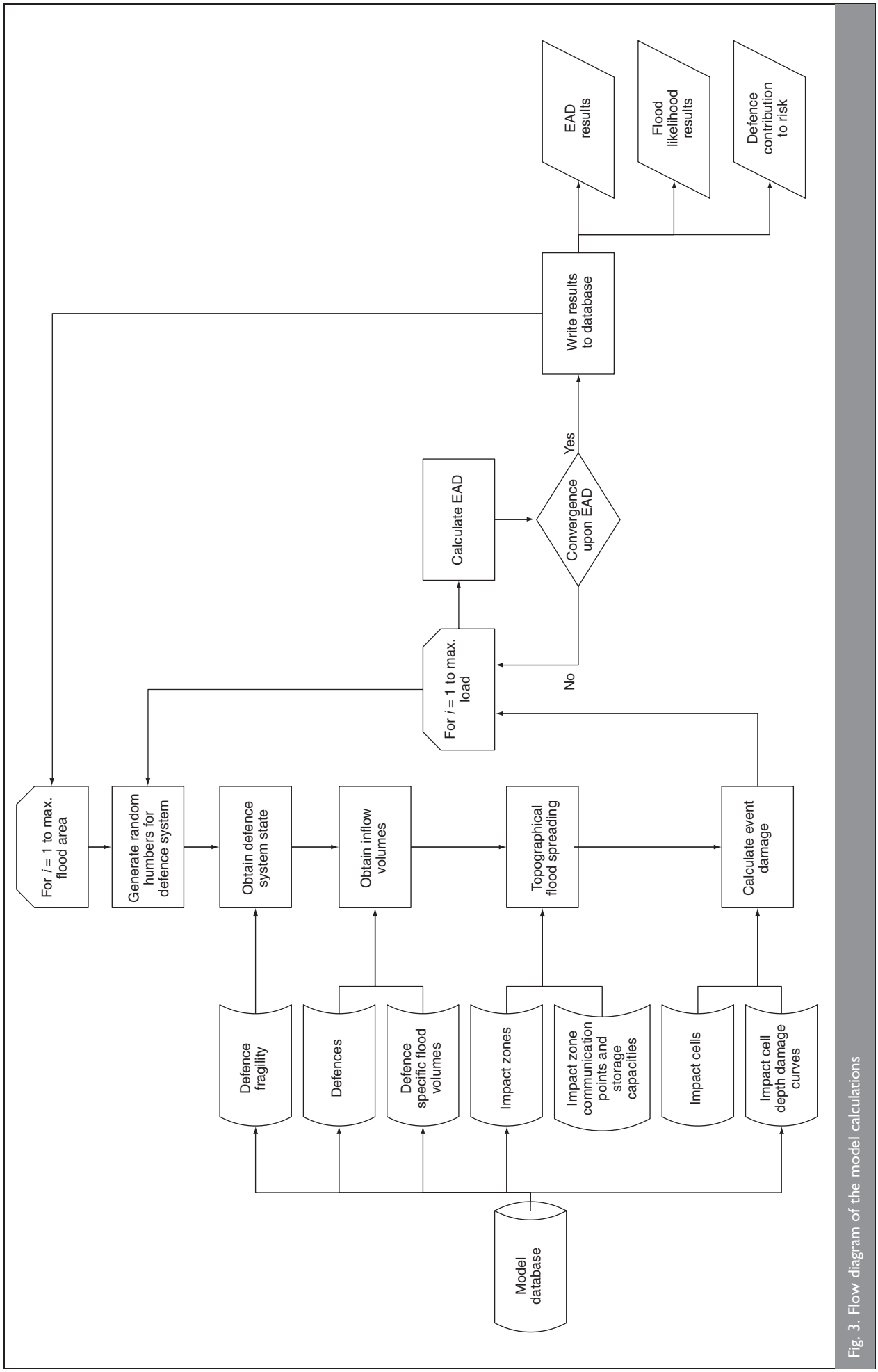

Fig. 3. Flow diagram of the model calculations

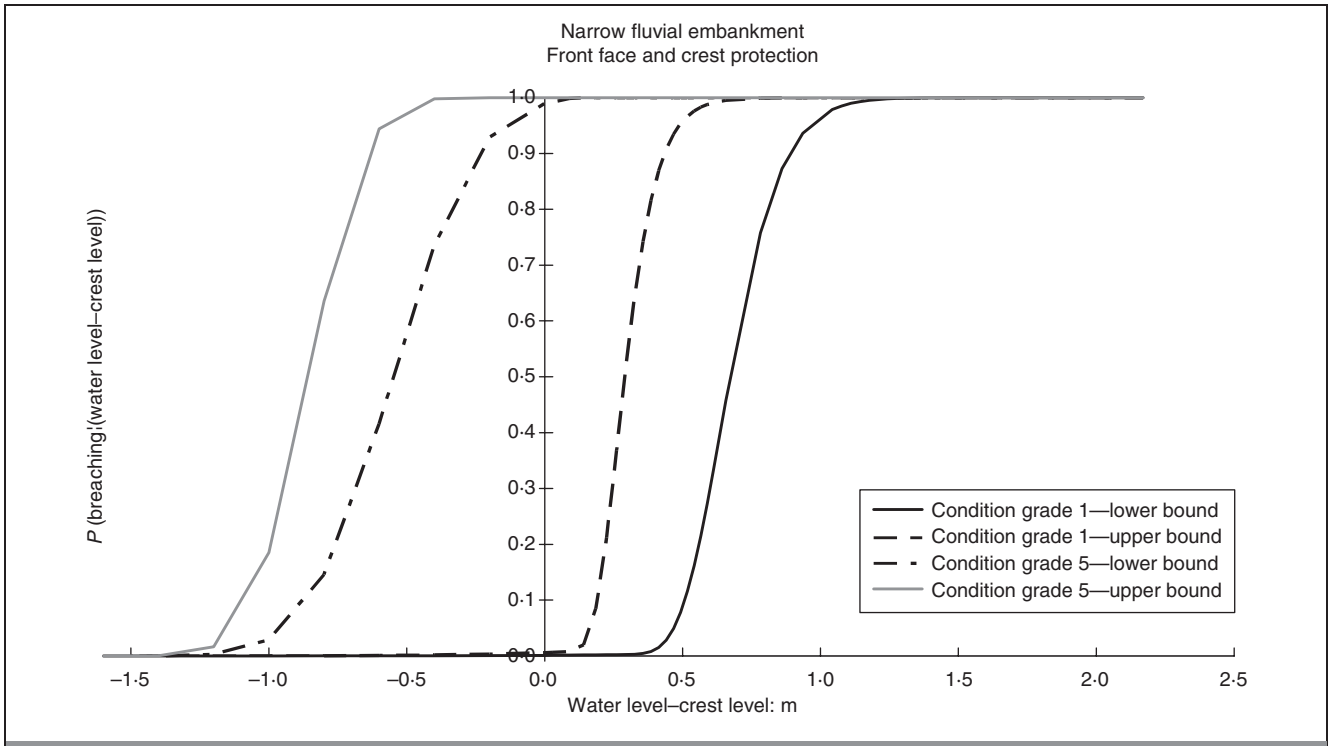

Fig. 4. Earth embankment defence fragility curves

approach is modified, the structural loads are treated as known deterministic variables. The probability of failure is then assessed over a plausible range of specified loading levels through integration of the joint density of the strength variables, over the failure region.

The generic fragility curves have been developed through consideration of two failure mechanisms: failure through piping, occurring where hydraulic pressure gradients arising from extreme fluvial water levels or sea levels cause seepage through defences, leading to internal erosion and collapse,[12,17] and failure owing to rear face erosion of the defence from overtopping.[12,18] A FORM method was used for integration of the resistance variables over the failure region.

As few data currently exist on the parameters of the limit state equations, their ranges and distribution functions have been assigned using expert judgement. The uncertainties introduced within the process are captured using upper and lower bound estimates (see Fig. 4).

4. FLOOD INUNDATION

4.1. Flood volume

The volume of water discharged into the floodplain from any defence section is obtained through first establishing a flow rate through or over the defence using a wave overtopping equation[19] or the broad crested weir equation.[20] Having established the flow rate, the volume of water discharging into the floodplain is then calculated assuming an appropriate event duration. This is typically based on hydraulically modelled flood event simulations that use observed flow rates (fluvial), or water level variations (tidal), for their boundary conditions. A number of uncertainties exist with regard to the input variables and parameters. These are included within the modelling process by assigning probability distribution functions and ranges to the inputs, based on site-specific data and/or expert judgement, this uncertain information is propagated through the volume calculation within a Monte Carlo procedure. The outputs of this process are probability distributions of volumes for each defence section for the q loading levels under failed and non-failed defence states. In practice, for computational efficiency, the expected volume for each loading level is propagated through the subsequent risk analysis.

4.2. Flood spreading method

There are numerous hydrodynamic models that can be used to simulate the propagation of flood water across floodplain areas. These models generally solve a form of the two-dimensional shallow water equations and range in complexity from raster-based approaches[21] that assume the flow between cells to be uniform and are based on the Manning equation, to more complex finite volume approaches that solve the full two-dimensional equations.[22] These models are computationally expensive to run, can suffer from instability problems and are time consuming to set up. Their application within the context of risk-based flood system models that require consideration of multiple breach and loading scenarios can be impractical. A rapid flood spreading method has therefore been developed that is computationally efficient yet is sufficiently robust for use in flood system risk models.

The model receives flood volumes discharged into floodplain areas from breached or overtopped defences and then spreads the water over the floodplain according to the encountered floodplain topography. The output from the model is a flood depth grid of the floodplain area. The model comprises two main elements, a pre-process and a hydraulic simulation.

The objective of the pre-process is to generate the model calculation mesh, which consists of a series of impact zones that

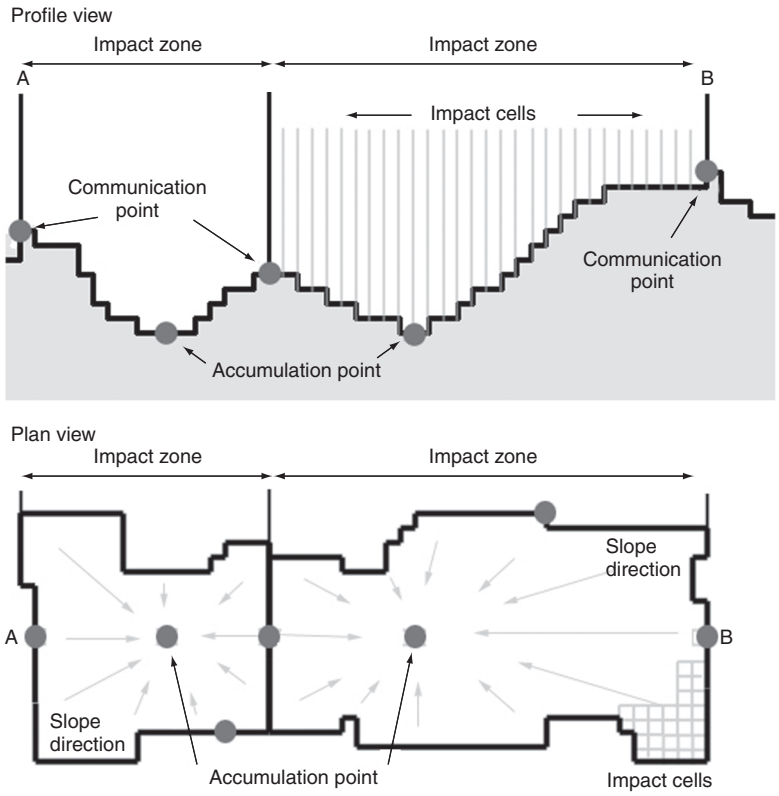

Fig. 5. Conceptual representation of impact zones and communication points

are based on the floodplain topography and therefore typically irregular in shape. Inputs to this process are the floodplain topography in the form of a digital elevation model (DEM) and the location of the defences relative to the DEM. Firstly, low points in the DEM (known as accumulation points, Fig. 5) are identified using a search algorithm. Then, the floodplain gradient extending outward from the accumulation point in eight separate directions is analysed. When a peak in the topography has been reached, impact cells located between the accumulation point and the peak are assigned to the accumulation point. All impact cells that are assigned to a single accumulation point form an impact zone (Fig. 5). An impact zone capacity database is constructed that contains the volume of water stored in an impact zone for different flood levels (Table 1). The impact cells that form the boundary between impact zones are then analysed and the cell with the lowest ground elevation along the boundary is recorded.

Impact zone number	Flood level: m above IZ ground level	Volume stored: m^3
1	1	0
1	1·2	100
1	1·3	200
1	1·35	400
1	1·4	650
1	1·5	1100
1	1·65	1600
1	1·7	1800
1	1·8	2300
1	1·9	2900

Table 1. Impact zone level–volume database

The level of this cell determines the point at which water flows between cells; this is known as a communication point (Fig. 5). The level at which an impact zone communicates with its neighbours is stored in a separate database (Table 2). The two databases comprise the output of the flood spreading pre-process.

For flood event hydraulic simulations, flood volumes (section 4.1) obtained from each defence length are discharged into their neighbouring impact zones (these are termed adjacent impact zones), which then become activated. The volume of water within an active impact zone is compared with the communication level (Table 1) and if a communication point is reached an excess volume is calculated and discharged into the appropriate neighbouring impact zone/s. This process is repeated, reducing the excess each time, until it is nil, thus conserving volume; the final flood depth grid is then obtained. The results obtained are a depth grid resolved to impact cell scale. The core algorithm of the hydraulic spreading method is depicted in Fig. 6. In order to validate the quality of the hydraulic simulations, the model has been compared with a hydrodynamic model that solves the two-dimensional shallow water equations over a range of different flooding scenarios. The simplified model proved to be a good approximation to the hydrodynamic model across the range of events,[23] with flood extents and flood depths within 15% of the hydrodynamic model. This type of storage cell method is, in common with the two-dimensional hydrodynamic models, most suited to modelling floodplains that have a relatively shallow gradient.

4.3. Attributing residual flood risk to defence assets

Effective flood asset management requires the targeting of limited resources to obtain the greatest benefit in terms of risk reduction. With systems of different defence types protecting floodplain infrastructure of varying economic values, located upon complex topography, it is often not apparent which defences within the system are the most important and hence a priority for maintenance intervention. Knowledge of the contribution to

Impact zone number	Communication level: m above IZ ground level	Neighbouring impact zone
1	1·35	2
1	1·7	3
1	1·9	4

Table 2. Impact zone neighbour database

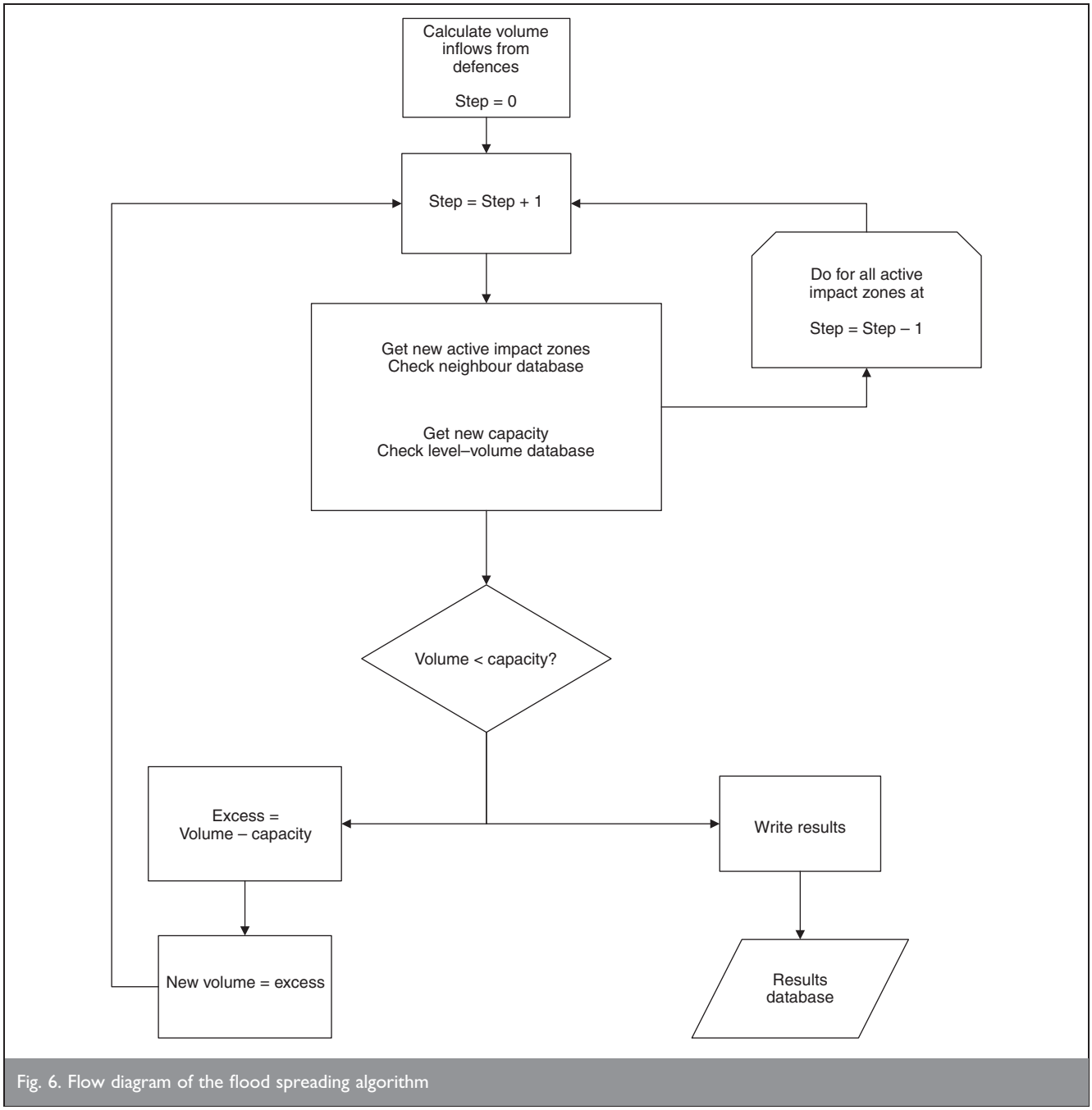

Fig. 6. Flow diagram of the flood spreading algorithm

residual risk made by specific defences can support the asset management process in these prioritisation decisions. This attributed risk represents the maximum possible reduction in risk that could be achieved through intervention measures such as crest raising or strengthening at that defence section; it is the reduction in flood risk that would arise if the defence were to be made infinitely high and strong. The methodology for attributing residual risk to defence sections involves establishing a relationship between the quantity of water discharged through each individual defence and the economic consequence of flood events. The vector comprising the defence system states can be sub-divided into sub-sets of defence groups. The defence sections in any defence group all discharge flood water into the same adjacent impact zone (IZ_j), for example

$$(\underbrace{d_1, d_2, d_3}_{IZ_i}, \underbrace{d_4, d_5, d_6, d_7}_{IZ_{i+1}}, \underbrace{d_8, d_9}_{IZ_{i+2}}, \underbrace{d_{10}, d_{11}}_{IZ_{i+3}}, \ldots, d_n) \quad (10)$$

Flood depths are a function of the defence system and also a function of flood volumes discharged through each of the defences $(v_1, v_2, \ldots, v_n)$

$$y = g_1(\underbrace{v_1, v_2, v_3}_{IZ_i}, \underbrace{v_4, v_5, v_6, v_7}_{IZ_{i+1}}, \underbrace{v_8, v_9}_{IZ_{i+2}}, \underbrace{v_{10}, v_{11}}_{IZ_{i+3}}, \ldots, v_n) \quad (11)$$

On each hydraulic flood simulation the proportion of flood volume contributed by each defence to each adjacent impact zone is obtained. Then, as the flood water propagates across the floodplain, the source adjacent impact zone is recorded and the quantity of water supplied to each destination impact zone is monitored. The flood event economic damage associated with each non-adjacent impact zone is then allocated to each of the adjacent impact zones according to the volume of water supplied. The total adjacent impact zone event damage is then apportioned according to the relative proportion of volume contributed by each defence. This

process is repeated on all flood event simulations and thus the residual risk can be attributed to each defence section. As knowledge of the defence system state is retained for each flooding scenario, it is possible to disaggregate this information further into risk arising from overtopping and breached flood events respectively. This can provide an indication of the most effective intervention measures, crest level raising or strengthening, for example. The performance of each defence section under different maintenance regimes can be measured in terms of risk reduction and benefit–cost analysis undertaken for each defence to provide an optimum investment strategy for risk reduction.

5. APPLICATION OF THE METHOD

5.1. Introduction to the Thames Estuary

The method has been applied in the context of a strategic flood risk management plan to assist in the economic appraisal of flood management options over the coming century. It should be noted that results presented here are preliminary only and are based on economic damage to existing property; future land use changes have been excluded. The final results of the economic appraisal may well differ significantly.

The Thames flood system is complex, it is subject to flooding from different sources, comprises a range of fixed and active structures, including the Thames Barrier, variable floodplain topography and assets with a wide range of value within the floodplain area. The primary source of flooding is from high sea levels (combinations of high astronomical tides and meteorological surges) propagating up the Thames Estuary. Extreme fluvial flows, however, can overtop defences, particularly in west London. The flood defences comprise a mixture of fixed linear defences as well as actively operated barriers and flood gates. The fixed defences range from, for example, vertical sheet pile walls to earth embankments. The active structures vary in their function. The Thames Barrier and other moveable barriers located on the River Roding (Barking Barrier), for example, are designed to limit the propagation extent

	Model input	LB—10th percentile	UB—90th percentile	Standard deviation/error	Distribution type
		Collected data			
Crest level	Basis: A Local GPS survey[†] B Low-level LIDAR[2] C Land charge register drawings 1997 D Statutory defence levels E Haskoning defence database F IA3 Condition inspection output G Version 1a model H Thames tidal database I Estimation from standard of protection	 −0·01 m −0·27 m −0·30 m −0·33 m −0·37 m −0·40 m −0·43 m −0·47 m −0·50 m	 +0·01 m +0·27 m +0·30 m +0·33 m +0·37 m +0·40 m +0·43 m +0·47 m +0·50 m	 0·0078 m 0·21 m 0·236 m 0·261 m 0·287 m 0·313 m 0·339 m 0·364 m 0·39 m	Normal
Load (values apply to loadings in estuarial areas and in tributaries)	Basis: Hydraulic modelling and expert judgement Return period: 1 10 100 1000 10000	 −0·02 −0·08 −0·20 −0·45 −0·82	 +0·02 +0·08 +0·20 +0·45 +0·82	 0·02 0·06 0·16 0·35 0·64	Normal
Ground level	Basis: High-level LIDAR	−0·54 m	+0·54 m	0·42 m	Normal
Defence length	Basis: NA	NA	NA	Assumed certain	NA
		Model parameters			
Weir equation constant	Basis: Physical model studies reported in the literature	−0·2	+0·2	0·16	Normal
Breach width multiplier	Basis: Literature/experience for example from EC Project IMPACT*	−0·5* Best estimate value	+ Best estimate value	NA	Triangular
Duration of overflow	Basis: Observed data and expert judgement.	−0·2* best estimate	+0·2* best estimate		Normal
Hydrograph multiplier	Basis: Observed data and expert judgement	−0·05	+0·05	0·039	Normal

[†]http://www.samui.co.uk/impact-project/impact_project_overview.htm

Table 3. Summary of uncertainty associated with inputs to flood volume calculations

of extreme sea levels. They therefore reduce the hydraulic loading conditions on upstream structures. Other active structures are designed to control flow of water directly into the floodplain area—the flood control gates at the entrance to King George V Docks, for example.

5.2. Application

The study area of interest was sub-divided into a series of flood areas. The boundaries of these areas were defined by naturally occurring divisions in the floodplain topography, typically areas of high ground and tributaries. The tidal boundary condition of the model was located at Southend in the outer estuary and the upstream fluvial limit was positioned at Teddington Weir (west London). A one-dimensional hydrodynamic model was used to imply a functional relationship (sometimes known as a structure or response function[24]) between peak values of the boundary variables and water levels within the estuary at a series of nodes corresponding to cross-sections of the hydraulic model. A joint probability method,[25,26] which involved extrapolation of the joint probability density of the boundary variables and the generation of a set of pseudo flood events through a Monte Carlo sampling technique, was then applied. The output of the analysis was a distribution of extreme water levels at each node within the estuary. Sets of extreme water levels occurring at different future epochs under different assumed climate change scenarios were then generated by simply re-scaling the pseudo boundary events for each epoch/climate change scenario and re-integrating over specific values of the response variable.

A defence database, which is compatible with the National Flood and Coastal Defence Database (NFCDD) but contains supplementary fields, was developed. The database was populated with data from, for example, NFCDD, Environment Agency areas, 'as-constructed' drawings and a light detection and ranging (LIDAR) survey. The discrete defence sections within the model were based directly on those in NFCDD (see also Fig. 2).

The extreme water level and defence crest level information was utilised in a probabilistic calculation of flood volume that also considered uncertainties in breach dimensions. Table 3 shows the

Deterioration—'Do nothing' scenario (P1)

		Best estimate Time (years) to reach condition from new					
Defence class	Description	Grade 1	Grade 2	Grade 3	Grade 4	Grade 5	(Grade 6)
4	Type 1, Narrow vertical wall, brick and masonry, front protection	0	5	15	25	30	40
5	Type 1, Narrow vertical wall, brick and masonry, front and crest protection	0	5	15	25	30	40
6	Type 1, Narrow vertical wall, brick and masonry, front, crest and rear protection	0	5	15	25	30	40
7	Type 1, Narrow vertical wall, sheet piles, front protection	0	10	20	30	40	60
8	Type 1, Narrow vertical wall, sheet piles, front and crest protection	0	10	20	30	40	60
9	Type 1, Narrow vertical wall, sheet piles, front, crest and rear protection	0	10	20	30	40	60
10	Type 2, Narrow embankment, turf	0	3	10	17	20	26
11	Type 2, Narrow embankment, rigid, front protection	0	9	19	29	38	56
14	Type 2, Narrow embankment, rip-rap, front protection	0	9	19	29	38	56
15	Type 2, Narrow embankment, rip-rap, front and crest protection	0	9	19	29	38	56
16	Type 2, Narrow embankment, rip-rap, front, crest and rear protection	0	9	19	29	38	56
20	Type 3, High ground	Not applicable to high ground cases					
21	Type 4, Culvert	0	6	13	19	26	40
30	Type 5, Narrow vertical wall, brick and masonry, front, crest and rear protection	0	6	13	19	*26*	*40*
31	Type 6, Narrow embankment, permeable revetments, front protection	0	6	13	19	*26*	*40*
34	Type 6, Narrow embankment, impermeable revetments, front protection	0	6	13	19	26	40
37	Type 7, Dune, beaches	0	8	13	18	26	42
38	Type 7, Shingle, beaches	0	8	13	18	26	42
42	Type 1, Wide vertical wall, brick and masonry, front and crest protection	0	5	15	25	30	40
45	Type 2, Wide embankment, turf	0	6	17	28	34	46
46	Type 2, Wide embankment, rigid, front protection	0	9	19	29	38	56
48	Type 2, Wide embankment, rip-rap, front protection	0	9	19	29	38	56
49	Type 2, Wide embankment, rip-rap, front and crest protection	0	9	19	29	38	56
57	Type 6, Wide vertical wall, brick and masonry, front and crest protection	0	6	13	19	*26*	*40*
59	Type 6, Wide embankment, permeable revetments, front and crest protection	0	6	13	19	26	40
60	Type 6, Wide embankment, impermeable revetments, front protection	0	5	10	15	20	30

Table 4. Deterioration rates for specified defence classes

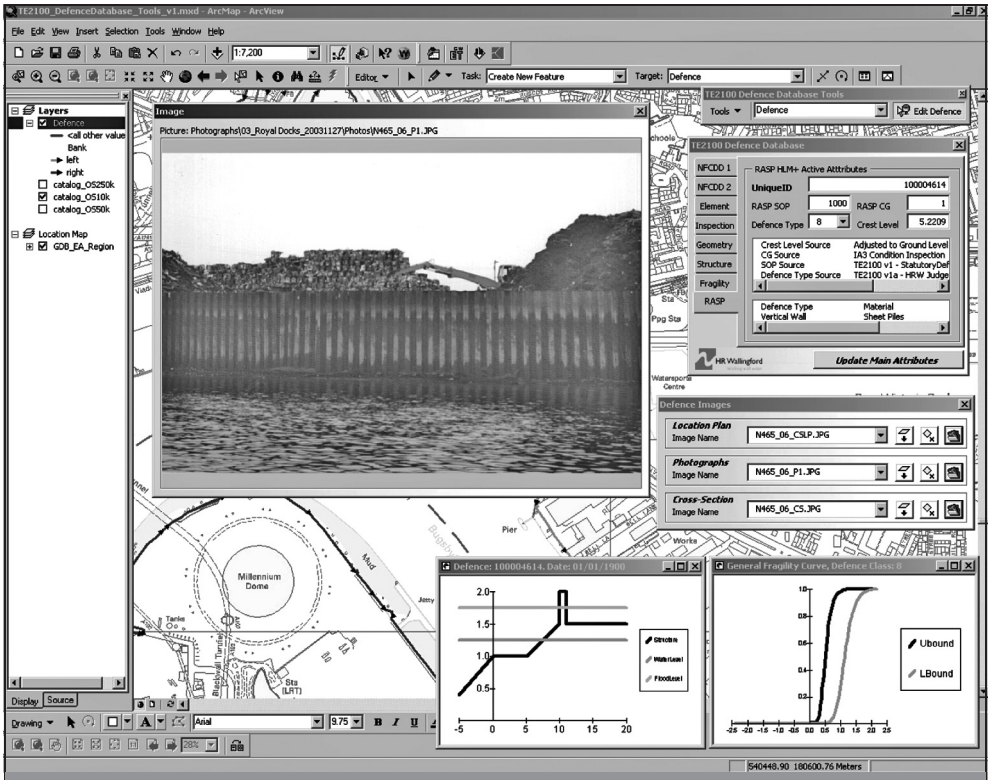

Fig. 7. Defence database

distribution functions and uncertain ranges on parameters that were input into a Monte Carlo simulation using the broad crested weir equation[20] to derive distributions of flood volumes for different defence types. The table shows how a data quality hierarchy from different sources of defence crest level has been used to inform uncertainty estimates.

A new inspection methodology,[27] focused on assessing the condition of structures in terms of their flood prevention performance, was applied and used to assign a performance rating (i.e. a condition grade) to a range of structure types over the study area. Deterioration of assets was represented through the elapsed time for defence types to increase in condition grade, derived through expert elicitation (see Table 4). A screenshot of the defence database is shown in Fig. 7. The geometry data and protection type were used together with a defence classification system[5] to assign each defence type a generic fragility curve. The performance of the active structures was incorporated within the model using fragility curves derived from structure-specific reliability analyses that consider human failure to operate the structures as well as mechanical failure[28] (see Fig. 8). Separate water level structure functions were constructed with the barriers in a failed state. The resultant risk, considering the barrier failure likelihood, was then derived by integration over the barrier failure states.

The impact zones for the flood spreading method were constructed using a 50 m regular grid obtained from LIDAR survey. Prior sensitivity analysis of flood event economic damage to grid size showed this was a reasonable grid resolution to use for the risk analysis. Example results from this analysis, for a nominal 100 year event with a breach simulated in the vicinity of the Royal Docks, are detailed in Table 5. Look-up tables of economic damage as a function of depth for each 50 m grid cell were constructed using the national property database (NPD) and standard values[14] for different residential and commercial property types (see Fig. 9). Although not currently implemented, it is evident that future land use changes, including increased floodplain urbanisation, can be reflected in this process and hence their impact on flood risk quantified.

The number of samples of the defence system state Monte Carlo procedure (section 2) was deemed sufficient when the EAD variation from successive batches (section 2) was within 1%. In a typical flood area this was reached after approximately 8000 flood spreading simulations. The computational time for a model run (i.e. to calculate EAD for all flood areas within the Thames Estuary system) was typically less than 1 h on a standard desktop personal computer. It is of note that the existing method for the national flood risk assessment takes in excess of 11 h computational time on an area of similar size.

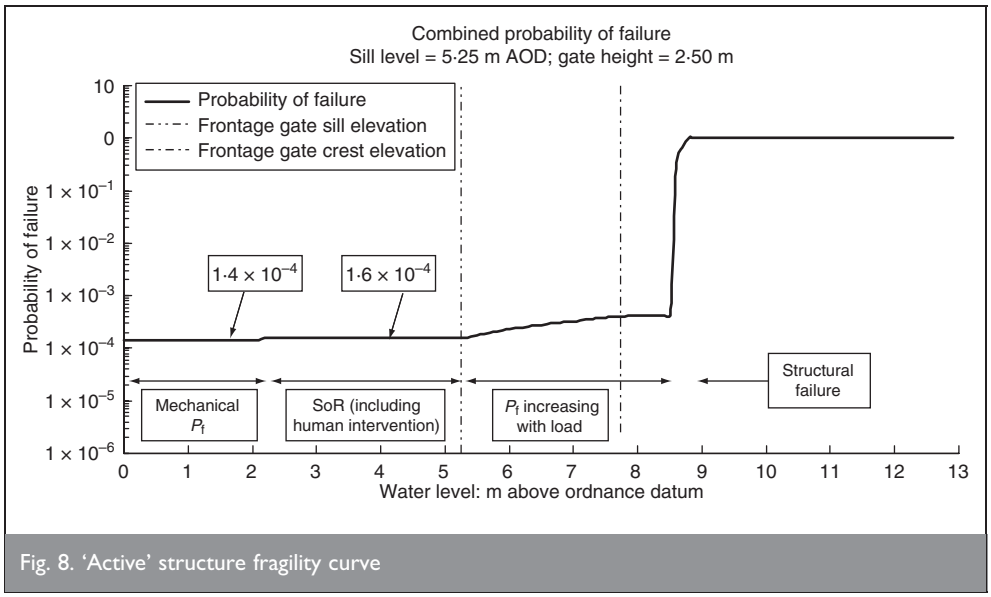

Fig. 8. 'Active' structure fragility curve

Model/grid size	Economic damage: £ million
Hydrodynamic model (100 m)	77·1
Rapid flood spreading model (100 m)	76·9
Hydrodynamic model (50 m)	75·4
Rapid flood spreading model (50 m)	74·6

Table 5. Sensitivity of flood event economic damage to model grid size

5.3. Results and discussion

The primary outputs for each model run are, for a specific epoch, floodplain economic risk and annual probability of inundation within each impact cell, defence contribution to residual risk and annual probability of defence failure. The analysis is prone to uncertainty owing to the limited data on many of the inputs. Uncertainty is handled explicitly and represented as upper and lower bands on the input fragility and depth damage relationships[14] determined with the support of expert judgement; these bands are propagated through the modelling system using a previously applied approach.[5] For the purposes of strategic long-term planning (preliminary economic appraisal), the model has been applied for the 'do nothing' (known as P1) and 'maintain existing' (known as P3) investment policies, over a number of future epochs and a range of climate change scenarios. The summary results of this analysis are presented in Fig. 10. The current present-day EAD is low, given the value of floodplain assets of over £60 billion, at £3·4 million

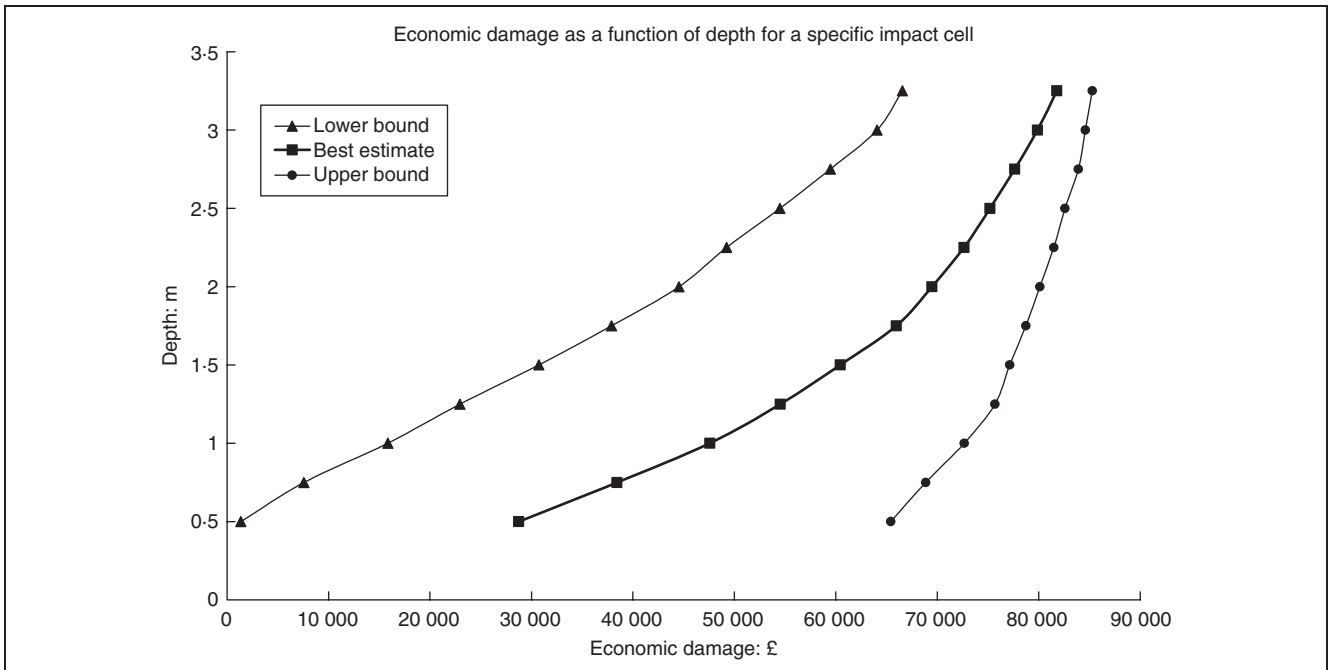

Fig. 9. Example depth damage curves for a single impact cell

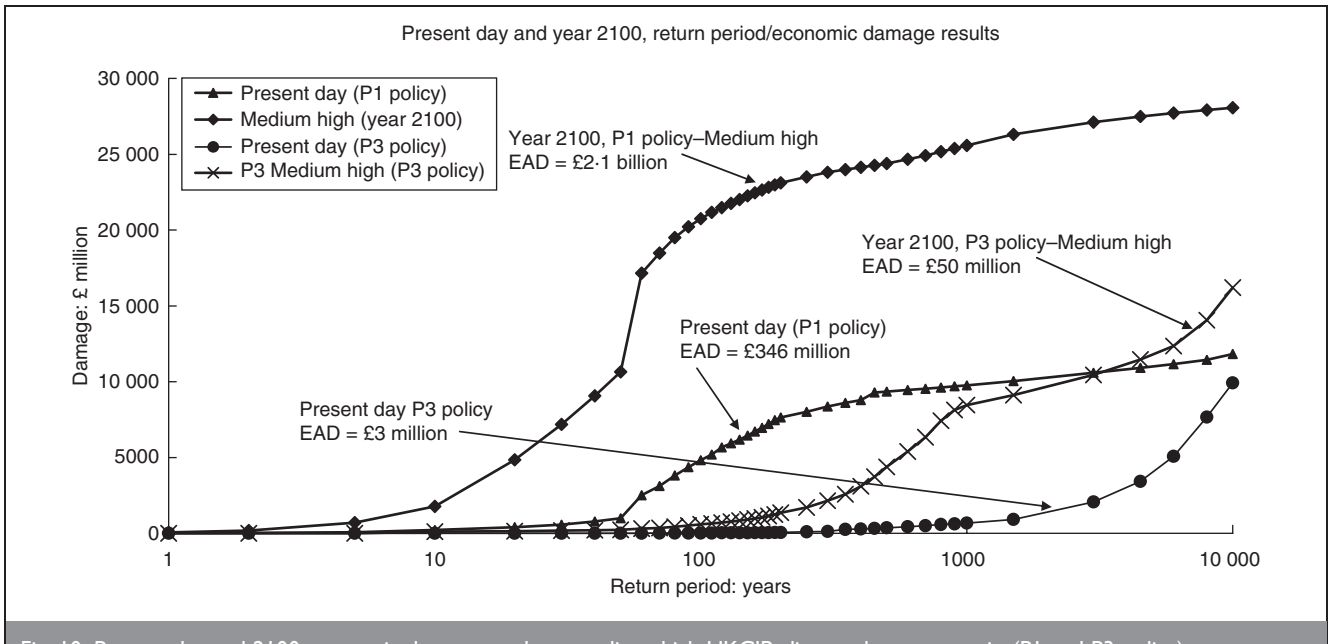

Fig. 10. Present day and 2100 economic damages under a medium–high UKCIP climate change scenario (P1 and P3 policy)

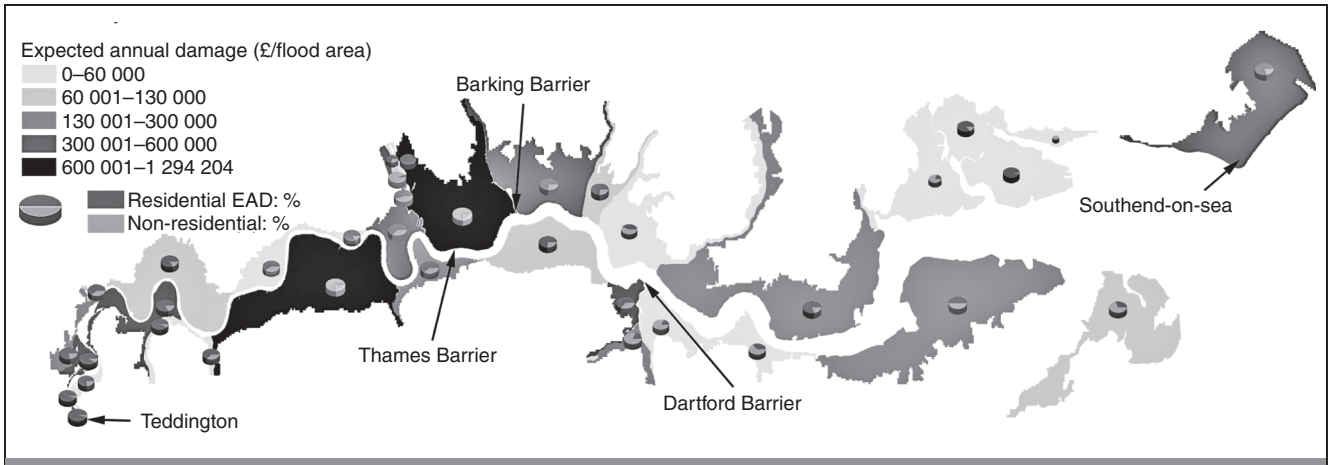

Fig. 11. Spatial distribution of EAD—maintain existing defence system

(lower bound = £2·8 million, upper bound = £4·3 million). This reflects the high design standards (>1000 year standard of protection) for much of the main estuary and the effectiveness of the active barriers, most notably the Thames Barrier. Events of significant economic damage only occur at return periods over 1000 years. The majority of risk within the inner estuary arises from flooding on the tributaries, with negligible risk arising from the Thames (Fig. 11). Such is the robustness of the current system that, were it maintained to its current levels of reliability, under a UKCIP medium–high climate change scenario[29] the increase in EAD is limited to approximately £50 million. Under the P1 policy when the barriers are not operated during flood events, the increase in risk is dramatic. Upstream of the Thames Barrier in Central London, there are certain locations that are flooded with a frequency of more than once every 10 years and significant areas flooded with a frequency of more than 100 years (see Fig. 12). The present-day EAD increases to approximately £350 million.

Table 6 shows the residual flood risk attribution for the top 20 contributing defences (P3 scenario), disaggregated into risk arising from breach and overtopping events respectively (subsequent to this analysis, these defences have been reviewed and, where necessary, works incorporated under the capital replacement programme). High values of the former indicate maintenance work to strengthen the structure is likely to prove cost effective, while intervention through crest raising is likely to prove prudent for defences with significant values of the latter. It is also interesting to note that approximately 70% of the risk stems from only 1% of the defences. Thus focused intervention in specific areas can yield significant benefits in terms of risk reduction.

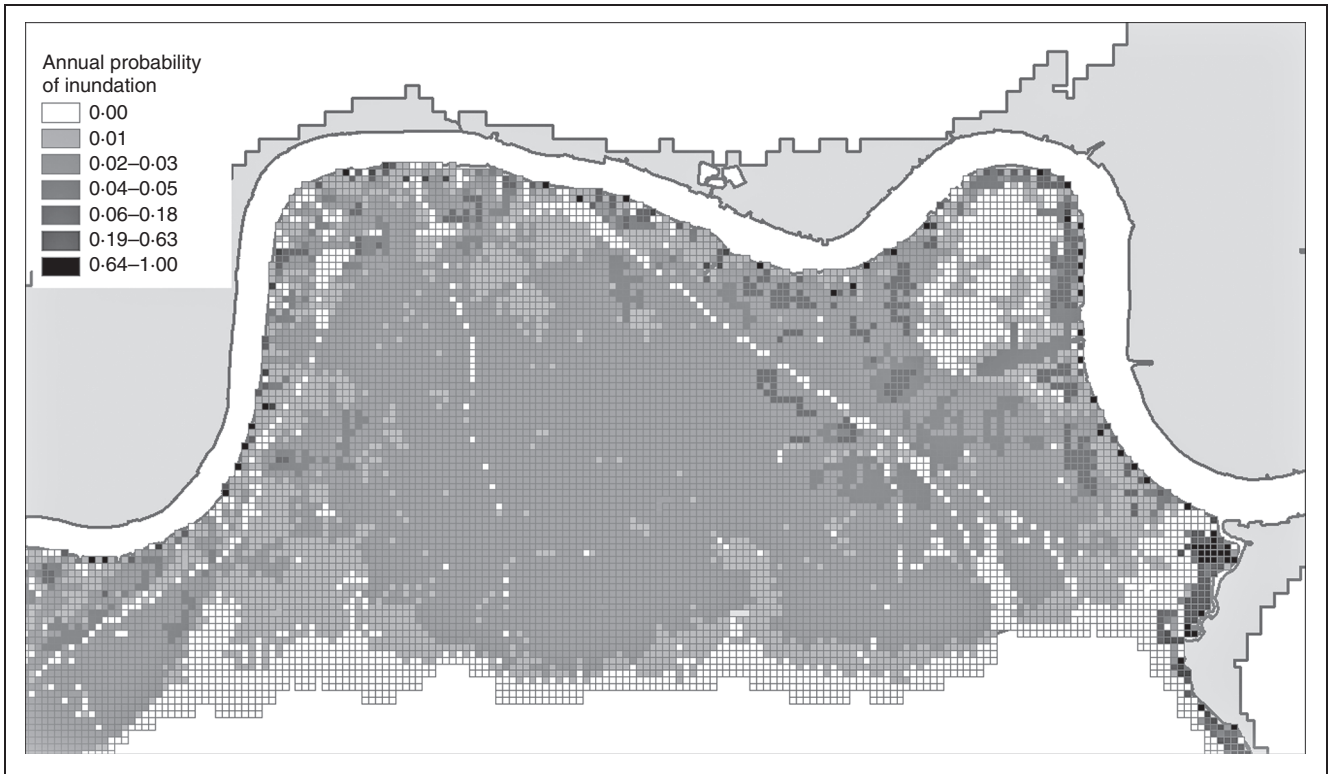

Fig. 12. Annual likelihood of inundation (P1 Policy)—Bermondsey

Defence unique identifier	Rank	Total contribution	Breach contribution	Overtop contribution
300005043	1	£334 601	£311 041	£23 560
300000014	2	£320 896	£0	£320 896
300005266	3	£166 306	£166 306	£0
300003265	4	£147 851	£147 851	£0
300000975	5	£142 233	£141 901	£332
300000926	6	£139 721	£0	£139 721
300001596	7	£115 803	£115 803	£0
300002431	8	£106 515	£364	£106 151
300000754	9	£102 060	£3 932	£98 128
300000007	10	£98 961	£95 964	£2 997
300005019	11	£79 216	£45 124	£34 092
300000920	12	£77 339	£0	£77 339
300004585	13	£75 830	£26	£75 804
300003352	14	£74 511	£50 524	£23 987
300001681	15	£73 386	£73 386	£0
300005254	16	£67 857	£67 857	£0
300001695	17	£63 973	£63 969	£4
300000332	18	£63 328	£0	£63 328
300000318	19	£62 659	£0	£62 659
300000477	20	£62 090	£32 023	£30 066

Table 6. Twenty defence sections with the highest attributed residual risk (P3 investment scenario)

6. CONCLUSIONS

The method detailed in the current paper represents a step change in the level of performance over traditional regional flood risk methodologies.[9] Defence failures are included and an efficient but robust flood spreading method is incorporated. Its application to the tidal Thames, a flood system of considerable complexity, demonstrates its robustness. It is evident that the range of outputs can be used to support a variety of flood management decisions and, although uncertainties can be significant, a relative comparison of different options can be made, with new approaches emerging for capturing the uncertainty within the context of robustness analyses. The model can be used to determine the risk reduction (benefit) afforded by different intervention strategies over their life cycle, which can then be compared with associated costs within a relative benefit–cost framework. Outputs of the system model related to specific defence sections can be used for asset management purposes, identifying where it is most cost effective to invest in defence maintenance and refurbishment.

While the model has been designed for regional-scale flood risk analyses, it is computationally more efficient and robust than the current national method. As it requires the same basic data, this method can potentially be used in place of the current national method. For regional-scale applications it is envisaged the model input data will be significantly improved over the national input data. For example, fragility curves based on site-specific analyses can be derived in preference to the generic curves. The model is most relevant for application in areas where raised defences are already prevalent, or where raised defences are being considered as part of a wider flood risk management strategy.

ACKNOWLEDGEMENTS

This work was funded by the Thames Estuary 2100 Project of the Environment Agency, the FLOODsite Project commissioned under the European Union's 6th Framework, the joint Defra/Agency research programme (Performance-based Asset Management), the Flood Risk Management Research Consortium, funded by EPSRC and the Environment Agency. The authors are particularly grateful to Owen Tarrant of the Thames Estuary 2100 project for the support provided to this work and to Graham Clark (WS Atkins) and Steve Newbold (Thames Estuary 2100, independent consultant) for provision of Fig. 7.

REFERENCES

1. Bye P. and Horner M. *Easter 1998 Floods*. Independent review team to the Board of the Environment Agency, Environment Agency, Bristol. Q3
2. Environment Agency. *Lessons Learnt*: *Autumn 2000 Floods*. Environment Agency, Bristol, ISBN 1857055063. Q4
3. Institution of Civil Engineers. *Learning to Live with Rivers*. Final report of the Institution of Civil Engineers Presidential Commission to review the technical aspects of flood risk management in England and Wales, Institution of Civil Engineers, London, 2001.
4. Sayers P. B., Hall J. W. and Meadowcroft I. C. Towards risk-based flood hazard management in the UK. *Proceedings of the Institution of Civil Engineers, Civil Engineering,* 2002, **150**, Special Issue No. 1, 36–42.
5. Hall J. W., Dawson R. J., Sayers P. B., Rosu C., Chatterton J. B. and Deakin R. A methodology for national-scale flood risk assessment. *Proceedings of the Institution of Civil Engineers, Water & Maritime Engineering*, 2003, **156**, No. 3, 235–247.
6. Evans E. P., Hall J. W., Penning-Rowsell E. C., Sayers P. B., Thorne C. R. and Watkinson A. Future flood risk management in the UK. *Proceedings of the Institution of Civil Engineers, Water Management*, 2006, **159**, 53–61. Q5
7. Seed R. B. *Preliminary Report on the Performance of the New Orleans Levee Systems in Hurricane Katrina on August 29, 2005*. ASCE, Reston, Virginia, 2005, Report UCB/CITRIS-05/01.
8. Bates P., Dawson R. J., Hall J. W., Horrit M. S., Nicholls R. J., Wicks J. and Hassan M. A. A. M. Simplified two-dimensional modelling of coastal flooding and example applications. *Coastal Engineering*, **52**, 793–810. Q6

9. Evans E. P., Ramsbottom D. M., Wicks J. M., Packman J. C. and Penning-Rowsell E. C. Catchment flood management plans and the modelling and decision support framework, 2002. *Proceedings of the Institution of Civil Engineers, Civil Engineering*, 2002, 43–48.
10. Environment Agency. *NAFRA 2005 Headline Results: Briefing Paper*. See http://www.environment-agency.gov.uk/commondata/acrobat/nafra_1432357.pdf for further details.
11. Centre for Civil Engineering Research and Codes and Technical Advisory Committee on Flood Defence. *Probabilistic Design of Flood Defences*. CUR, GOUDA, 1990.
12. HR Wallingford. *Performance and Reliability of Flood and Coastal Defences*. HR Wallingford, 2005, Environment Agency Research and Development Technical Report 2318/1.
13. HR Wallingford. *Risk Performance and Uncertainty in Flood and Coastal Defence*. HR Wallingford, 2002, Environment Agency Research and Development Report FD2302/TR1, HR Wallingford Report SR587.
14. Penning-Rowsell E., Johnson C., Tunstall S., Tapsell S., Morris J., Chatterton J. and Green C. *The Benefits of Flood and Coastal Risk Management; A Manual of Assessment Techniques*. Middlesex University Flood Hazard Research Centre, 2005.
15. Buijs F., Sayers P. B. and Gouldby B. P. *Preliminary Reliability Analysis on the Thames*. EU FLOODsite Project, 2007, Report T07-07-02.
16. Melchers R. E. *Structural Reliability Analysis and Prediction*, 2nd edn. Wiley, New York, 1999.
17. Terzaghi K. and Peck R. B. *Soil Mechanics in Engineering Practice*, 3rd edn. Wiley, New York, 1996.
18. Vrouwenvelder A. C. W. M., Steenbergen H. M. G. M. and Slijkhuis K. A. H. *Theoretical Manual of PC-Ring, Part A: Descriptions of Failure Modes*. Nr. 98-CON-R1430, Delft, 2001.
19. Environment Agency. *Wave Overtopping of Sea Walls: Design and Assessment Manual*. Environment Agency, 1998, Research and Development report W5/006/2.
20. Chadwick C. and Morfett J. (eds). *Hydraulics in Civil and Environmental Engineering*, 3rd edn. Spon Press, London and New York, 2002.
21. Bates P. D. and De Roo A. J. P. A simple raster-based model for flood inundation simulation. *Journal of Hydrology*, 2000, **236**, 54–77.
22. Alcrudo F. and Mulet-Marti J. Urban inundation models based upon the Shallow Water equations. Numerical and practical issues. *Proceedings of Finite Volumes for Complex Applications IV*, Hermes Science Publications, 2005.
23. HR Wallingford. *Rapid Flood Spreading Methodology (RFSM)*. Environment Agency, 2006, Thames Estuary 2100 Report, DT4.
24. Rajashekhar W. R. and Ellingwood B. R. A new look at the response surface approach for reliability analysis. *Structural Safety*, 1993, **12**, 205–220.
25. Hawkes P. J., Gouldby B. P., Tawn J. A. and Owen M. W. The joint probability of waves and water levels in coastal engineering design. *Journal of Hydraulic Research*, 2002, **40**, no. 3.
26. Coles S. G. and Tawn J. A. Statistical methods for multivariate extremes: An application to structural design. *Applied Statistics*, 1994, **43**, 1–48.
27. Long G. and Mawdesley M. *Improved Approaches to Condition Assessment—Volume 1: Performance-Based Visual Inspection of Flood Defence Assets*. Flood Risk Management Research Consortium, University of Nottingham, 2006, Report UR10, Vol. 1.
28. Clark G. and Newbold S. Thames Estuary 2100: asset management studies of 'active' tidal cefences on the Thames Estuary. *Proceedings of the 42nd Defra Conference, York*, 2007.
29. Hulme M., Jenkins G. J., Lu X., Turnpenny J. R., Mitchell T. D., Jones R. G., Lowe J., Murphy J. M., Hassell D., Boorman P., McDonald R. and Hill S. *Climate Change Scenarios for the United Kingdom: the UKCIP02 Scientific Report*. UK Climate Impacts Programme, 2002.